EXPERIMENTAL LQR-BASED ANFIS CONTROL FOR DOUBLE-LINKED INVERTED PENDULUM ON CART

Truong-Phuong-Nam Pham [1], Huy-Minh-Quan Ha [1], Truong-Nhat-Minh Bui [1], Pha-Phim Nguyen [1], Anh-Huy Nguyen [1], Duc-Cuong Vu [1], Van-Dat Nguyen [1], Hai-Thanh Nguyen [2]*

[1] Ho Chi Minh City University of Technology and Engineering (HCM-UTE)
Vo Van Ngan Street, No. 01, Ho Chi Minh City (HCMC), Vietnam
[2] Nguyen Huu Canh Technical and Economics Intermediate School
500-502, Huynh Tan Phat St., HCMC, Vietnam
* Corresponding author. E-mail: nguyenhaithanh@nhct.edu.vn

Abstract: Double inverted pendulum on cart (DIPC) is a high-order single input-multi output (SIMO) model. Due to its challenges in balancing control, there are less experimental results on this model. This paper extends our previous LQR experiments on the double inverted pendulum on cart (DIPC) by introducing an ANFIS-based LQR controller. Experimental results show enhanced stability and robustness under nonlinear dynamics, confirming the effectiveness of combining optimal control with intelligent learning methods.
Keywords: Double inverted pendulum, SIMO system, ANFIS, Underactuated System, Experimental Validation.

1. Introduction

The double-linked inverted pendulum on cart (DIPC) extends the classical inverted-pendulum benchmark to a higher-order, underactuated, and strongly nonlinear setting. Small disturbances can rapidly drive the links away from the upright configuration, and chaotic behaviors may emerge without precise stabilization. Owing to these challenges, DIPC is widely employed to assess advanced control strategies—optimal, robust, and intelligent—and remains closely related to practical systems such as robotic manipulators, legged platforms, and aerospace stabilization mechanisms [1–3]. Foundational surveys and historical overviews further reinforce its status as a canonical testbed in nonlinear control [1, 2].

To stabilize such a SIMO, multivariable system, a broad spectrum of approaches has been explored, ranging from conventional PID and fuzzy schemes to model-based optimal control. Among these, the Linear Quadratic Regulator (LQR) stands out for its rigorous design and strong local guarantees around the upright equilibrium. LQR implementations on cart–pole variants have demonstrated high-accuracy balancing under suitable modeling and linearization, although performance can degrade in the presence of unmodeled nonlinearities, parameter drift, and sensor/actuator imperfections that are typical in hardware deployments [4-6].

Hybrid intelligent strategies have been proposed to enhance adaptability while preserving the structure of optimal control. The Adaptive Neuro-Fuzzy Inference System (ANFIS) combines rule-based fuzzy reasoning with data-driven learning, enabling nonlinear input–output mapping and adaptive tuning from measured data or reference responses [7]. Prior studies on inverted-pendulum families indicate that ANFIS-based controllers can improve robustness and disturbance rejection relative to purely linear designs, motivating ANFIS–LQR hybrids for underactuated systems [8, 9].

Building upon our prior work—where the DIPC model was formulated via forward kinematics and an ANFIS-based LQR scheme was validated in simulation [10], we observed that cart-position regulation in simulation remained insufficiently tight for both LQR and ANFIS controllers. In a subsequent study [11], we refined and experimentally implemented LQR on a DIPC platform, obtaining stable and accurate performance. Leveraging these two foundations, the present paper advances to an experimental ANFIS-based LQR realization on DIPC, aiming to transfer intelligent control to a complex nonlinear plant and to quantify improvements in response and disturbance rejection over a purely linear baseline. This progression establishes a practical pathway toward deploying intelligent optimal control on more complex underactuated systems.

2. DIPC Model

To analyze the system and derive its motion characteristics, it is first necessary to establish the mathematical model of the double-linked inverted pendulum on cart (DIPC). The overall configuration of the system is illustrated in Fig. 1, where the reference coordinate frames are defined. These coordinate frames serve as the reference basis for the DIPC, enabling the application of kinematic modeling techniques commonly used in robotics theory [13]. The resulting kinematic equations provide the foundation for further analysis and dynamic modeling of the system behavior. Detailed

procedures for the modeling and derivation process are presented in [10], [11].

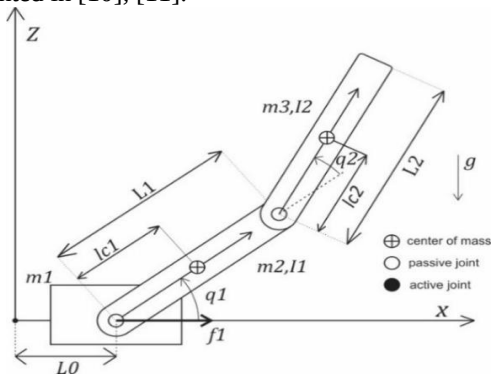

Fig. 1. Structure of the system [10]

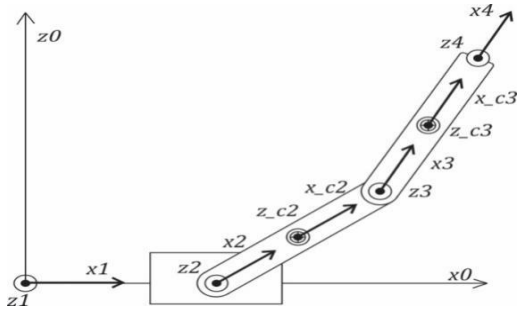

Fig. 2. Axis system of joints in the system [10]

3. ANFIS Controller

3.1. ANFIS Training Loop [9]

Consider a training set of K input–output pairs:

$$\{(x(1),d(1)),...,(x(k),d(k))\} \quad (1)$$

Step 1: Select the learning rate $\eta \succ 0$ and the maximum cumulative error $E_{\max}$.

Step 2: Initialization: set $E=0$ and assign initial values to the nonlinear parameters $\theta_N(0)$.

Step 3: Estimate the linear parameters θ_L via least squares by minimizing.

$$\sum_{k=1}^{K}\left[d(k)-H(x(k),\theta_N(0))\theta_L\right]^2 \to \min \quad (2)$$

$$\Rightarrow \theta_L=\left[\sum_k H^T H\right]^{-1}\left[\sum_k H^T d(k)\right] \quad (3)$$

Step 4: Update θ_N using gradient descent over samples k=1,…,K:

Error:

$$E(k)=\frac{1}{2}\left(d(k)-H(x(k),\theta_N)\theta_L\right)^2 \quad (4)$$

Update:

$$\theta_N(k)=\theta_N(k-1)+\eta\frac{\partial E(k)}{\theta_N} \quad (5)$$

Accumulate:

$$E=E+E(k) \quad (6)$$

Step 5: If $E \prec E_{\max} \to terminate$, otherwise reset $E=0$ and repeat from Step 3 for the next training epoch.

3.2. LQR-based ANFIS Controller

The design of the LQR and ANFIS controller has been presented in detail in studies [10] and [11]. In this paper, we build upon that foundation to develop an ANFIS controller.

In our previous study [10], the LQR controller had not been fully optimized, resulting in suboptimal cart position performance. In the subsequent study [11], we employed a Genetic Algorithm (GA) to determine a more optimal gain matrix K, which significantly improved the stability of the cart position.

$$K=\begin{bmatrix} 0.9763 \\ 4.9193 \\ -30.8268 \\ -15.2867 \\ -136.3463 \\ -24.7514 \end{bmatrix}^T \quad (7)$$

Based on these results, the LQR controller data obtained from [11] were utilized to train an Adaptive Neuro-Fuzzy Inference System (ANFIS). The data acquisition and training procedure was described in [10]. Building on that methodology, we trained the ANFIS for both simulation and experimental studies. The dataset comprises approximately 10,000 samples with a sampling period of 0.005 s, using six DIPC state variables as inputs and one control signal applied to the cart as the output. Gauss membership functions (*gaussmf*) were adopted. Training was conducted with Matlab 2020a's anfisedit, and convergence was achieved after 80 epochs when the error ceased to change appreciably. The structure of the ANFIS controller designed for the DIPC system is illustrated in Fig. 3.

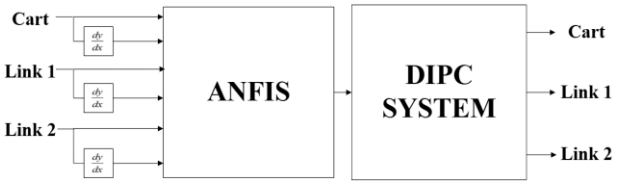

Fig. 3. ANFIS control structure

With six input variables and three membership functions assigned to each input, the resulting neuro-fuzzy controller consists of $3^6 = 729$ rules, as illustrated in Fig. 4. The response surface of the ANFIS controller between the input variables and the output is shown in Fig. 5.

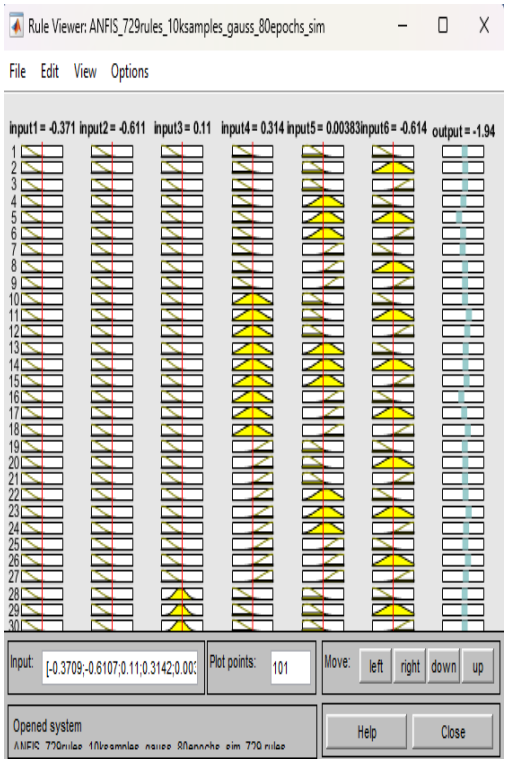

Fig. 4. 729rules of ANFIS controller

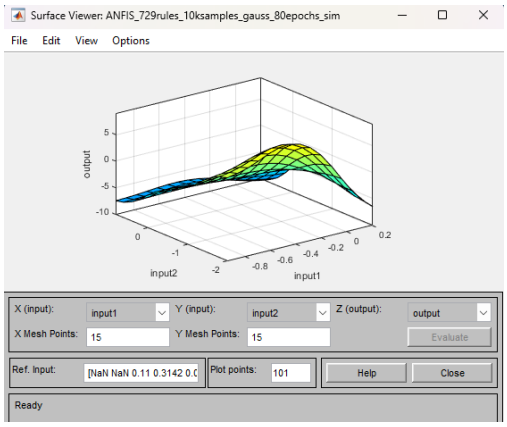

Fig. 5. ANFIS response surface

4. Simulation Results

To bridge the gap between simulation and real-world implementation, the state variables were fed back by emulating the actual signal reading process of the physical encoder. This approach enables a more accurate assessment of the system's stability under practical conditions. The detailed implementation of the encoder model in the simulation environment has been presented in [10] and [11].

The simulation environment was developed in Matlab 2020a Simulink with a sampling period of 0.005s, is illustrated in Fig. 6, which is identical to that used in the real system.

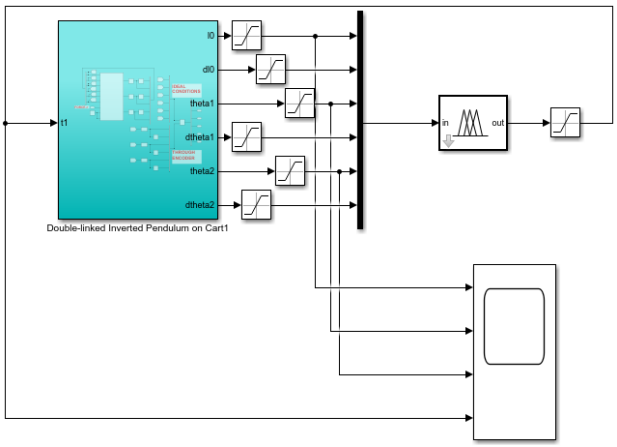

Fig. 6. Simulation of DIPC with an ANFIS controller

The initial value of the deviation angle of link 1 is set to 0.1 rad (~5.7°), while the deviation angle of link 2 is initialized at 0.15 rad (~8.6°).

From the cart position response shown in Fig. 7, it can be observed that, since the two pendulums initially deviated from their equilibrium positions, the actuator generated a large force to pull the system back to its steady operating point. As a result, the cart exhibited significant oscillations at the beginning, then gradually stabilized with an amplitude of approximately ±0.2 m - a reasonable and safe range. Notably, the ANFIS controller outperformed the LQR controller by reducing the cart's overshoot (0.8 m compared to 0.95 m), indicating that the ANFIS successfully learned from the LQR data and even achieved better performance.

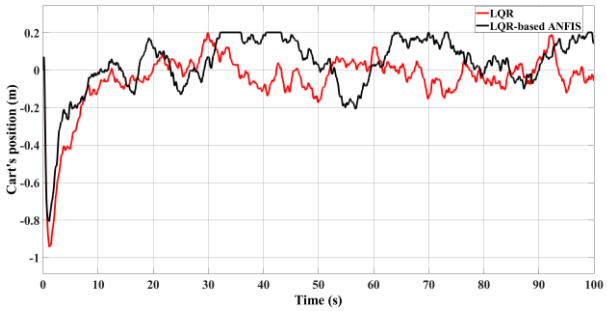

Fig. 7. The cart position response

Fig. 8 and Fig. 9 illustrate the angular responses of pendulum 1 and pendulum 2 under reduced-resolution conditions, as previously mentioned. The oscillation amplitude of the first pendulum is mostly within the range (−0.05, 0.04) rad, while that of the second pendulum remains within (−0.02, 0.02) rad. Both pendulums exhibit highly stable responses; if these results were obtained under real conditions, they would represent excellent performance, demonstrating the success of both the ANFIS and LQR controllers in stabilizing the DIPC system.

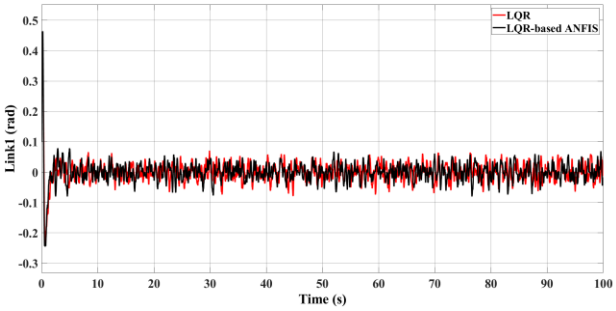

Fig. 8. The first pendulum's response

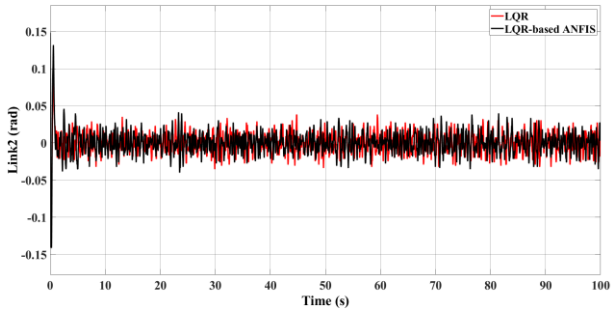

Fig. 9. The second pendulum's response

The force was converted into torque [11] by multiplying it with the pitch radius of the pulley to estimate the torque acting on the system. In Fig. 10, the torque amplitude ranges from −0.13 to 0.13 N·m. These results provide a useful basis for hardware evaluation and adjustment to meet the system's performance requirements.

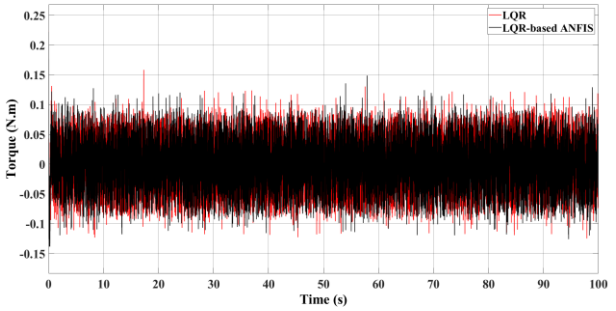

Fig. 10. Applied torque on the cart

Overall, the ANFIS controller effectively learned from the LQR data to balance the DIPC system in the simulation environment. This result provides a solid foundation for further development and implementation of the algorithm on the experimental setup.

5. Experiment Results

We chose the Trimf membership function for the real DIPC system because it provides clear rules, efficiently divides the control space, and ensures stability, especially with 729 rules.

The hardware setup [11] employed in this study is illustrated in Fig. 11 and Fig. 12 as follows:

1. Motor's encoder.
2. Link 1 and its encoder.
3. Link 2 and its encoder
4. NISCA DC motor.
5. Pulley transmission mechanism.
6. STM32F407G-DISC1.
7. BTS7960 H-Bridge circuit.
8. Encoder signal reading and UART circuit.
9. Power circuit breaker.

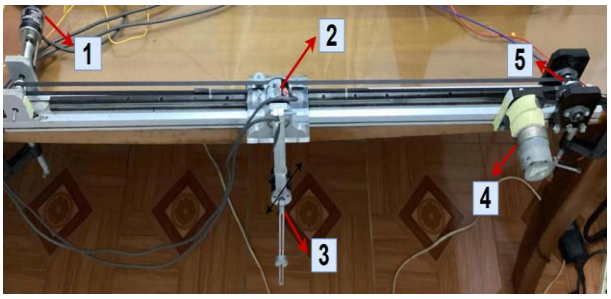

Fig. 11. Hardware setup of the DIPC system [11]

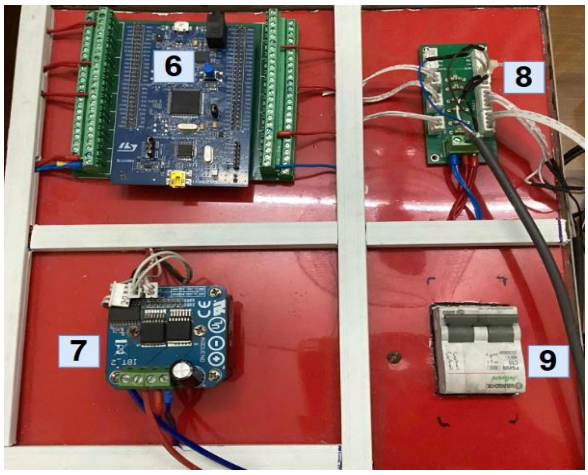

Fig. 12. Control circuit for the DIPC system [11]

Fig. 13 illustrates the hardware connection diagram of the practical DIPC system. Fig. 14 illustrates the processing flow of the DIPC system control program.

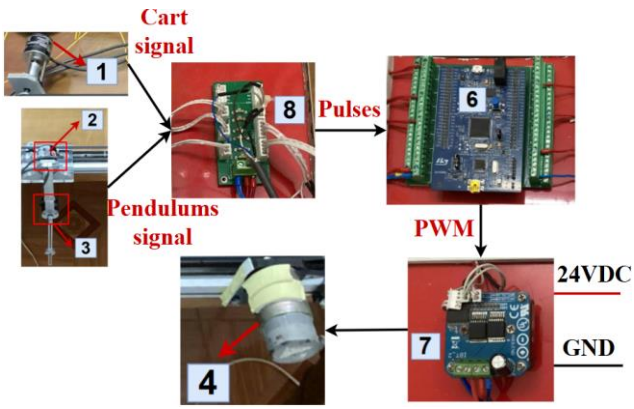

Fig. 13. Connection diagram [11]

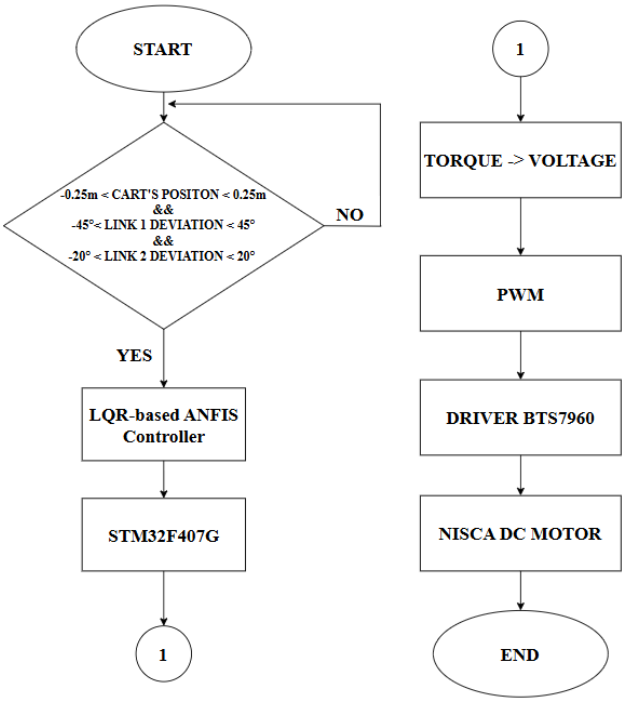

Fig. 14. Algorithm flowchart for DIPC system [11]

This section presents a comparative analysis of the experimental performance of the DIPC system under the LQR controller [11] and the LQR-based ANFIS controller.

Fig. 15 illustrates the experimental response of the cart's position. It is evident that both the LQR and LQR-based ANFIS controllers successfully maintain the cart's oscillation within a tight boundary, approximately (-0.05, 0.05)m. Notably, the practical position response for both controllers is superior to the results obtained during simulation. Although both methods prove effective, the ANFIS controller demonstrates slightly superior performance, exhibiting a better capability to restore the cart to the equilibrium position and maintain its stability compared to the LQR controller

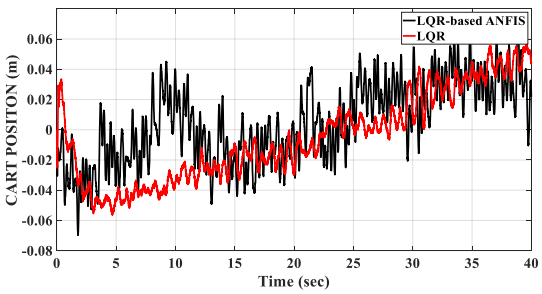

Fig. 15. Experimental response of cart position

Fig. 16 and Fig. 17 present the experimental angular deviation responses for the first and second pendulums, respectively. These results indicate that the ANFIS controller successfully learned the dynamics from the LQR data, demonstrating a stable balancing capability for both links. Although the angular oscillation amplitude under ANFIS is slightly larger than that of the LQR, these oscillations were observed to be minor during practical operation. This amplitude is considered fully acceptable, enabling smooth and stable real-world performance of the system.

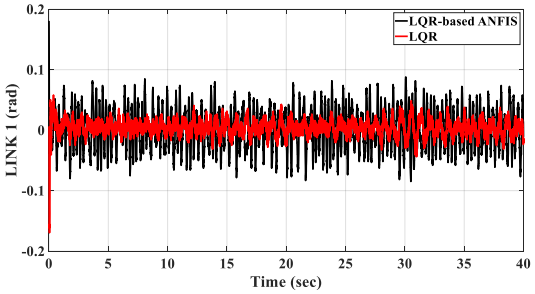

Fig. 16. Experimental response of the first pendulum angle

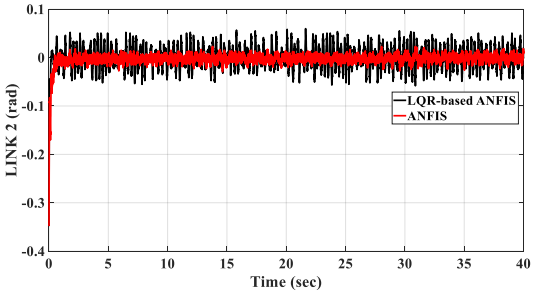

Fig. 17. Experimental response of the second pendulum angle

Fig. 18 and Fig. 19 illustrate the motor torque responses. Based on these torque values, we applied the conversion equation presented in [11] to transform the torque into the corresponding voltage. As observed from both figures, the control force generated by the LQR controller is significantly larger than that of ANFIS, to the extent that the ANFIS data are almost overshadowed on the same scale. This explains why, during real operation, the LQR-controlled system produces noticeably louder mechanical noise, whereas the ANFIS controller demonstrates superior efficiency in optimizing control energy, resulting in smoother and quieter system performance

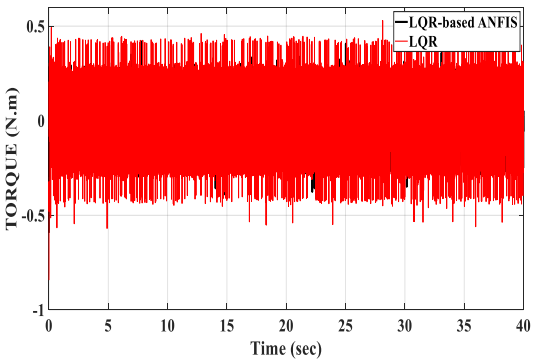

Fig. 18. Actual torque acting on the cart

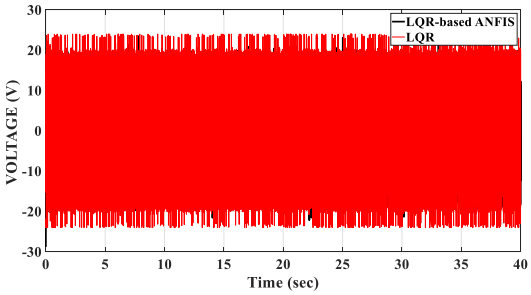

Fig. 19. Actual voltage supplied to the motor

Table 1 below presents the RMSE values used to quantitatively and visually evaluate the system responses under the ANFIS and LQR controllers, providing further support for the observations discussed above.

Table 1. Quality of DIPC according to the Root Mean Square Error Standard

Response of system	Controller	
	LQR	ANFIS
Cart (m)	0.0299	0.0267
Link1 (rad)	0.0144	0.036
Link2 (rad)	0.0135	0.0246
Voltage (V)	13.6137	17.0216

6. Conclusions

In this study, we successfully implemented the intelligent ANFIS controller on the experimental DIPC system - a highly nonlinear and complex setup. The experimental results demonstrated excellent performance, with the pendulum angle responses closely matching the simulation outcomes. Similar to the LQR-based study [11], the cart position in the experiment achieved even better performance than in simulation. Notably, the ANFIS controller provided smoother operation due to its adaptive and efficient modulation of the control signal.

These findings establish a solid basis for further optimization of the system's performance in terms of both state response and energy efficiency in future research. Furthermore, the experimental framework will be expanded to incorporate advanced control strategies such as trajectory tracking and nonlinear control, paving the way for deeper exploration of intelligent control algorithms for the DIPC system.

Acknowledgement

This research was funded by Ho Chi Minh City University of Technology and Engineering (HCM-UTE). We also want to give thanks to PhD. Van-Dong-Hai Nguyen (HCMUTE) due to his supervision to complete this research. We, authors, are grateful for these supports.

7. References

[1] Lundberg K.H., Barton T.W.: "History of Inverted-Pendulum Systems", IFAC Proceedings, Vol. 42, No. 24, pp. 131–135, 2010.
[2] Boubaker O.: "The Inverted Pendulum Benchmark in Nonlinear Control Theory: A Survey", Inverted Pendulum – New Trends, Applications and Control, InTechOpen, London, 2013.
[3] Irfan S., Zhao L., Ullah S., Mehmood A., Butt M.F.U.: "Control Strategies for Inverted Pendulum: A Comparative Analysis of Linear, Nonlinear, and AI Approaches", PLoS ONE, Vol. 19, No. 3, 2024.
[4] Yadav S.K., Sharma S., Singh N.: "Optimal Control of Double Inverted Pendulum Using LQR Controller", Int. J. Adv. Res. Comput. Sci. Softw. Eng., Vol. 2, No. 2, pp. 189–192, 2012.
[5] Yaren Y., Kizir S.: "Energy-Based Modeling and LQR Controller Design for Cart–Pole Double Inverted Pendulum", Proc. Int. Conf. Systems and Control (ICSC), pp. 1–6, 2021.
[6] Vi-Do Tran et al: "Balancing control for double-linked inverted pendulum on cart: simulation and experiment", Journal of Technical Education Science, Vol. 12, No. Special Issue 02, pp. 68–75, 2017.
[7] Jang J.-S.R.: "ANFIS: Adaptive-Network-Based Fuzzy Inference System", IEEE Trans. Systems, Man, and Cybernetics, Vol. 23, No. 3, pp. 665–685, 1993.
[8] Qiang S., Zhou Q., Gao X.Z., Yu S.: "ANFIS Controller for Double Inverted Pendulum", Proc. 6th IEEE Int. Conf. Industrial Informatics, pp. 475–480, Daejeon, 2008.
[9] Nguyen C.-H. et al: "ANFIS-Based LQR Control for Rotary Double Parallel Inverted Pendulum", Journal of Fuzzy Systems and Control, Vol. 2, No. 2, pp. 109–116, 2024.
[10] Pham T.-P.-N. et al: "An LQR-Based ANFIS Control for Double-Linked Inverted Pendulum on Cart", Journal of Fuzzy Systems and Control, Vol. 3, No. 2, pp. 135–141, 2025.
[11] Truong-Phuong-Nam Pham. et al: "Experimental LQR Control for a Double-Linked Inverted Pendulum on Cart", Journal of Science and Transport Technology, In Progress.
[12] Tran T.-B. et al: "A Survey of Identification Experimental System Parameters Using Genetic Algorithm", Robotica & Management, Vol. 29, No. 1, pp. 39–44, 2024.
[13] Craig J.J.: "Introduction to Robotics: Mechanics and Control", Pearson Education Inc., Upper Saddle River, NJ, 2005.